Integration of a Breadboard Power Conditioner with a 20-cm Ion Thruster

T. D. MASEK,* T. W. MACIE,* AND E. N. COSTOGUE*
Jet Propulsion Laboratory, Pasadena Calif.

AND

W. J. MULDOON,† D. R. GARTH,‡ AND G. C. BENSON§
Hughes Aircraft Company, El Segundo, Calif.

A breadboard of a lightweight 2.5-kw power conditioner was developed and integrated with an oxide ion thruster. The power conditioner was subsequently modified and integrated with a hollow cathode thruster. The problems of integration with each type of thruster are reviewed. Work leading to optimization of the closed-loop system performance during startup and recycling after thruster arcing is described. Electrical efficiency, weight, reliability, and other critical parameters are evaluated. The integration program has shown that the system satisfies the requirements of solar electric spacecraft.

Introduction

A SOLAR electric propulsion (SEP) system must perform two basic functions. The first is to efficiently convert available solar power into thrust power by accelerating ionized propellant to high velocity. The second function is to provide control torques for maintaining spacecraft three-axis attitude control. The Solar Electric Propulsion System Technology (SEPST) Program at JPL is directed toward establishing the technology at all system elements relating to these two functions. The program objectives and element status throughout the development process have been described in numerous papers.[1-6] The present paper deals with the integration of the most recently developed power conditioner (PC) unit with a 20-cm-diam, 2.5-kw thruster. Previously tested PC units have been reported.[4,5]

The area of major difference between past PC units and the one described here should be emphasized. Distinct differences exist in regulation for input voltage variation, minimization of input line ripple, packaging for a thermal-vacuum environment, and weight. In addition, despite the increased complexity due to line regulation and ripple requirements, the efficiency and reliability are expected to be improved over previous units.

The subject PC unit is designated BB-1 to indicate a breadboard status. PC design and fabrication was carried out at Hughes Aircraft Company under contract to JPL, with integration and testing at JPL.

Development of BB-1 was accomplished in two steps. Based on an existing oxide cathode thruster technology, an original BB-1 was designed, integrated, and tested for over 1300 hr. The last 500 hr of this testing was "hands off" operation. At that point, a suitable hollow cathode thruster, promising longer life and higher efficiency, had been developed. The PC unit was then modified to the BB-1M configuration to operate the hollow cathode thruster. This paper will briefly review the oxide cathode thruster PC design, integration, and testing experience. The major portion of the paper will focus on the hollow cathode thruster PC work.

Detailed studies of the PC operating characteristics with the thruster include recycle during arcing, input and output ripple, servo loop performance, and efficiency. Factors affecting recycle such as the magnet ramp duration, minimum magnet current, high-voltage turn-on sequencing, and discharge current level are discussed. Two experimental units, EX-1 and EX-2, were delivered in Jan. 1971 and have been integrated. The results of this work will be presented in a future report.

Power Conditioner Design

The application of SEP to near-term spacecraft requires all system elements to meet efficiency, weight, and reliability constraints. The performance goals for the present power conditioner units, based on previous designs are: 1) efficiency greater than 90%; 2) specific weight less than 5.0 kg/kw (of nominal output power); and 3) calculated reliability greater than 0.95 for 10,000-hr operation. A number of general requirements should be presented to place these goals in perspective.

First, most interplanetary missions are characterized by variable solar array power and variable solar array output voltage. The conditioning of the raw solar power must consider this voltage variation. The lightest and most efficient conditioning approach is to provide input line regulation within the PC.[7] Use of a separate line regulator is not acceptable for meeting the over-all system performance goals. Regulation over a 2 to 1 voltage range (40–80 v) was provided in the BB-1 (oxide cathode) unit and over a 1.5 to 1 range for BB-1M.

The second major requirement is on packaging. The PC weight must include allowance for heat rejection and launch vibration loads. The present PC units, like the previous Hughes Aircraft Company units built for the JPL SEP program, are designed for self-radiation to black space. While this appears to be the optimum PC configuration, it does impose certain constraints which must be recognized in the spacecraft design.

Third, the current and voltage ripple induced upon the solar array power buss must be minimized. It is believed that ripple at frequencies below 50 kHz will affect the array voltage.[8] For such cases, a margin of power must be provided in the solar array design to take care of the peak ripple power. The present PC specification allows less than 5% ripple on input current.

Presented as Paper 71-159 at the AIAA 9th Aerospace Sciences Meeting, New York, January 25-27, 1971; submitted March 5, 1971; revision received October 26, 1971. This paper presents the results of one phase of research carried out in the Propulsion Research and Advanced Concepts Section at the Jet Propulsion Laboratory, California Institute of Technology, under Contract NAS 7-100, sponsored by NASA.

Index category: Electric and Advanced Space Propulsion.

* Member of the Technical Staff. Member AIAA.
† Senior Staff Engineer. Member AIAA.
‡ Group head.
§ Member of the Technical Staff.

Fourth, the current state-of-the-art in high-efficiency, high-power electronics restricts the design to the use of transistors. Equivalent thyristor (SCR) PC technology is about a year behind the transistor units.[9]

These four basic requirements have produced a design that is characterized by the following features: 1) a synchronized, pulse-width-modulated, staggered-phase drive for multiple inverter modules, to reduce input and output filter weight and EMI. 2) The use of high-voltage (400-v collector-emitter open circuit), high-current (20amp), high-speed silicon transistors (Solitron SDT-8805 on BB-1, Transitron ST-18037 on EX-1, EX-2) stressed up to one-half the maximum rating in current and in voltage. 3) An extension of converter frequency to 10 kHz for d.c.-d.c. converters. The frequency of 10 kHz was chosen to minimize the combined transistor and transformer losses. (Transistor losses increase while transformer losses decrease with frequency.) 4) The extensive use of high Curie point ferrites for power transformer cores. 5) A thermally self-sufficient design, requiring no supplementary radiator, resulting in a large-area, low-height geometry. 6) Use of thermally self-sufficient functional modules, eliminating low-thermal impedance, high-weight transfer of heat before direct radiation to space. (A low thermal surface density of 0.04 w/cm^2 is used for 25°C radiator temperatures.) 7) Mounting of dissipative components directly on the final radiator, reducing the weight of component mounting. 8) A high-strength, low-weight, dip-brazed aluminum, "egg-crate" structure to support functional modules, permitting edge mounting of the PC structure to the spacecraft, with minimum weight in the spacecraft structure. 9) A low-voltage stress, both dielectric and surface, for high-voltage circuitry, made possible by large-area, low-density packaging. 10) A high level of functional circuit redundancy, made possible by use of low-power (250 w) inverter modules with a total maximum power output capability of approximately 3 kw. 11) Use of redundant, standby inverters for high system reliability. 12) Extensive use of integrated circuit digital and analog components.

Hollow Cathode System (BB-1M)

The oxide cathode system (BB-1) is described in Ref. 10, and only the modified breadboard (BB-1M) is discussed here. Oxide cathode life limitations required the thruster and PC to be modified to a hollow cathode (HC) configuration. The requirements to which the BB-1M unit was designed are shown in Table 1. The supplies modified or added to accommodate the hollow cathode are PS3, 4, 9, and 10 (Fig. 1).

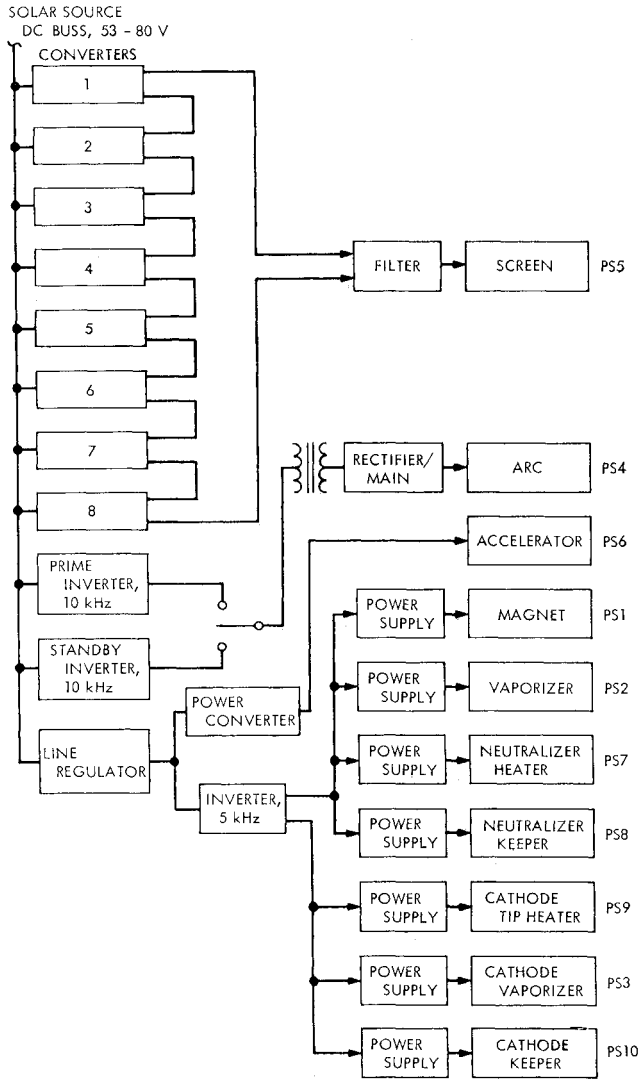

Fig. 1 Hollow cathode power conditioning unit.

Table 1 PC power requirements (hollow cathode, 20-cm thruster)

PS no.[a]	Supply name	Type	Maximum rating			Nominal rating			Regulation	Peak ripple, %	Range of control, amp
			E, *V*	*I*, *A*	*P*, *W*	*E*, *V*	*I*, *A*	*P*, *W*			
1	Magnet manifold	d.c.	19	0.85	16	13	0.6	8	±1%(*I*)	5	Constant current
7	Neutralizer heaters	a.c.	12	3.4	40	5.2	1.5	8	Loop or ±5%(*I*)	...	0.3–3.4
8	Neutralizer keeper	d.c.	300 at 5 ma[b]	1.0 at 0	10	10	0.5	5	±5%(*I*) at 15 v	2	0.1–0.5
9	Cathode heater	a.c.	8.5	4.8	40	8.5	4.8	40	5%(*I*)	...	On/off
10	Cathode keeper	d.c.	300 at 5 ma[b]	1.0 at 0	10	10	0.5	5	±5%(*I*) at 8 v	2	...
2	Vaporizer, main	a.c.	10	2	20	5.5	1.1	6	Loop or ±5%(*I*)	...	0–2
3	Cathode vaporizer	a.c.	10	2	20	5.5	1.1	6	Loop or ±5%(*I*)	...	0–2
4	Arc	d.c.	60 at no load	37.5 at (9 + 1) amp	375	37	(8 + 1)	333	±1%(*I*)	2	2–10
5	Beam	d.c.	2200[c]	1.05	2100	2000	1.0	2000	±1%(*E*)	5	0.5–1.0
6	Accelerator	d.c.	1100[c]	0.05	50	1000	0.01	10	±1%(*E*)	5	...

[a] Group I: PSI, 7–10; Group II: PS2, 3–6.
[b] 30 v at 20 ma.
[c] No load voltage.

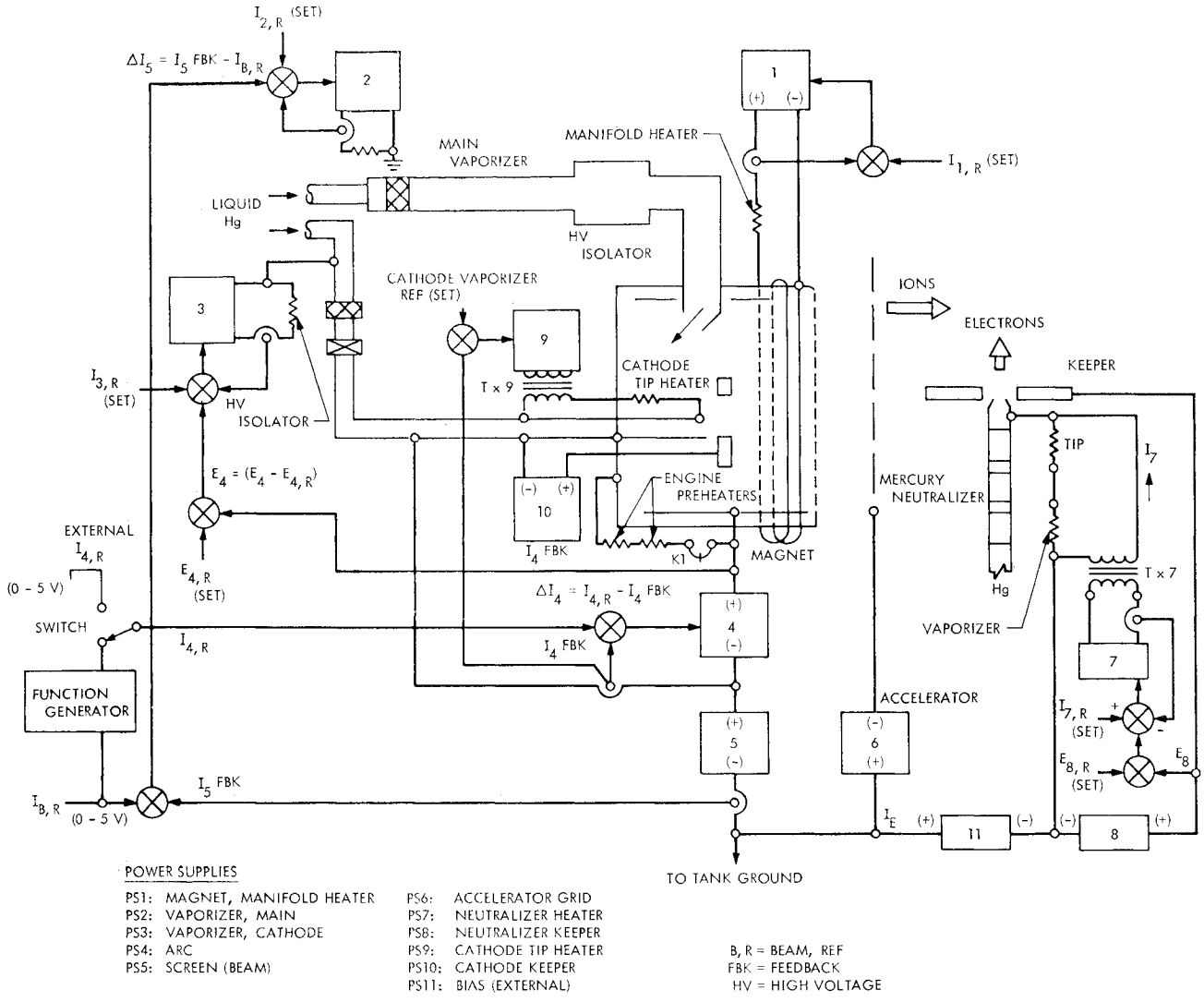

Fig. 2 20-cm-diam HC thruster PC control loops.

To accommodate hollow cathode thruster requirements, the arc supply had to be increased in output power capacity at low line. To avoid having to completely reconfigure the system, while maintaining standby redundancy, an increase in the low line voltage from 40–53 v was accepted. The reduced input voltage range resulted in a somewhat higher PC efficiency and did not substantially affect the design. A block diagram of the **BB-1M** unit is shown in Fig. 1 and the PC-thruster servo loop configuration is shown in Fig. 2. The supply modifications will be reviewed briefly.

The screen power supply consists of eight d.c.-d.c. converters that operate staggered by 22.5° and deliver up to 2 kw of beam power to the thruster. With an input voltage of 53v, a failure of any two converters can occur without derating the output power. At an 80-v input, operation at full power is possible with four failed inverters.

The increased minimum input voltage allowed a single arc supply to produce 375w (10 amp maximum, including screen current), while maintaining a standby inverter. On BB-1 at a 40-v input, only 300w was available. The BB-1M arc supply is current-limited with arc voltage control from the HC vaporizer.

The accelerator supply is a single inverter delivering -1000 v d.c. at a nominal current of 5ma. The nominal steady-state power level of 5w gives this supply a very high calculated reliability. For this reason, a redundant inverter was not considered necessary. No output regulation is necessary because power is delivered from the line regulator source and the output voltage is affected only slightly by the load variation.

The 5-kHz inverter output power was increased to accommodate the new HC supplies (cathode heater, cathode keeper, and cathode vaporizer). This was accomplished by the increased minimum input voltage, which allowed a higher output voltage from the line regulator. The 5-kHz inverter was modified to provide two outputs. One output supplies the original modules (magnet, main vaporizer, neutralizer keeper, and neutralizer heater) at 70v peak. The second output, at 96v peak, supplies the hollow cathode modules.

The BB-1 control module was modified to provide for the arc voltage-cathode vaporizer control loop, thruster on/off commands, and recycle procedure changes. In addition, a runaway circuit was added to prevent thruster operation at low-propellant utilization.

Based on the EX-1 design, with only minor changes from the BB-1M unit, a reliability of 0.95 for 10,000 hr is predicted. The total parts count for the EX-1 unit is approximately 1500.

Integration Testing

A. Thruster

Although the thruster is well characterized electrically by the PC specifications (Table 1) and the PC-thruster integration data to be presented in later sections, the cathodes and

general configuration should be discussed briefly. The 20-cm-diam oxide cathode thruster used in testing BB-1 has been reported in detail.[2,11] The power efficiency was about 81% at 80% propellant utilization efficiency. Thruster operation and control are relatively easy with the oxide cathode. However, the oxide cathode life is limited to less than 1000 hr. Because of life requirements of 5000–10,000 hr for typical missions, an alternate cathode was chosen.

The hollow cathode has been under development for several years and was flight tested on SERT II.[12] This cathode is expected to meet the life requirement and improve thruster efficiency.

Details on the configuration, operation, and performance data for this basic design have been reported.[5] The power efficiency, including neutralizer, is about 86% at 88% propellant utilization efficiency.

B. BB-1 (Oxide Cathode) Integration

The principal function of any integration testing is to determine areas of interaction and evaluate the consequences of the interactions. In most cases, this becomes a period of evaluating failures or design weaknesses. In testing the BB-1 unit, the goal was to evaluate the general applicability of the design techniques and components for flight prototype use.

Integration and evaluation of the BB-1 unit took place between July and November 1969. Details of this testing phase have been reported,[10] but the major results will be summarized here. The principal difficulties resulted from transient voltage spikes penetrating into integrated circuit wiring and power lines. The spikes resulted from high current surges during thruster arcing. Both logic malfunctions and component failures occurred.

The signal return ring, which is a common point for low voltage and telemetry signals, was initially connected in series with the screen and accelerator power return. The high current surges (up to 300 A) generated by the screen and/or accelerator arcs passed through the signal return. Voltage transients up to 300v (with respect to the facility ground) were observed on the signal returning. Although the integrated circuits were designed to float with the signal return, capacitance between the integrated circuits and the circuit mounting plate allowed noise penetration. To eliminate this noise problem, the signal and power returns were separated and inputs to sensitive portions of the logic filtered. Specific details of the procedure for turning off the PC during thruster arcing (to prevent power supply damage) and re-establishing normal operation have been reported.[10]

In the first period of testing, prior to eliminating the noise problem, about 800 hr of PC-thruster operation was accumulated. Most (95%) testing was at full power with over 10,000 recycles counted. After all the modifications were introduced, the closed-loop system was operated for an additional 500 hr. During this period, the system performed satisfactorily with no manual intervention required. In this second testing period, operation was also at full power and an additional 10,000 recycles occurred. This demonstrated that the cures introduced were satisfactory. The 500-hr run was terminated voluntarily after it was felt that sufficient confidence had been gained in the performance and reliability of the improved circuits to warrant their acceptance.

C. BB-1M (Hollow Cathode) Integration

This integration period had a somewhat different emphasis from that of the original BB-1. The emphasis of BB-1 testing was primarily on thruster-PC compatibility, with basic performance evaluation and investigative testing only as needed. The BB-1M testing was extended to include the evaluation of the PC performance. This included testing of compatibility with the total SEP system as well as fundamental PC operating characteristics, capabilities, and limitations.

1. Startup

The hollow cathode thruster, when used in a fully integrated multiple-thruster array, requires a relatively long and orderly startup program which must be implemented in the power conditioner. Basically, the required startup sequence is the result of thermal packaging constraints as well as thruster starting characteristics.

To minimize condensation, heating elements were added to the isolator, feedline, and thruster backplate. These are connected in series with a thermal switch and the anode terminal. The arc power supply is used for preheating. When the terminal switch opens at about 175°C, the heaters are removed from the arc supply circuit, which is then fully available to power the discharge.

Once the discharge has been initiated, it can be sustained without power fed to the hollow cathode tip heater. Since this is desirable both from cathode lifetime and from power conservation viewpoints, the hollow cathode tip heater power is cut off automatically after the discharge current reaches about 4 amp.

The startup sequence is implemented by means of a series of externally generated commands. As given in Table 2, the internal commands are generated within the control logic of the PC by arc current level detectors.

The ON-1 command initiates the preheating of the thruster by turning on the supplies indicated. During this period, the manifold is preheated by PS1, the isolator and the feedline of the main vaporizer, as well as the backplate of the thruster, are preheated by PS4, and the tip of the hollow cathode is preheated by PS9. Supplies PS8 and PS10 are idling.

When the thermal switch opens at 175°C, both vaporizers are turned on by the ON-2 command. The low magnet current is established by the ON-3 command, which at the same time starts the high-voltage supplies PS5 and PS6. After the arc current has reached a preset value of 3–5 amp, and the screen and accelerator currents have been established, the magnet is automatically raised to the nominal 0.62 amp level. At the same time, the cathode tip heater is automatically turned off. With the use of this procedure, thruster full-power operation can normally be achieved after 30–60 min.

2. Neutralizer

In order to achieve steady operation, for most tests, an electron source outside the thruster was required. Without such a source, the PC operation was erratic with relatively noisy power outputs. This resulted in frequent accelerator spikes and recycles. Similar effects were observed in previous work.[5]

3. Recycle

The screen and accelerator power supplies are protected by a "trip" circuit against overloads. The current transient required to trip these supplies is plotted in Fig. 3 as a function of the transient duration. These characteristics also existed on BB-1. The procedures studied for reinitiating high voltage, without causing overshoots which could trip the system again, will be presented here.

The major factor in "soft" recovery from a trip is the magnetic field strength. During a recycle, the magnet current is

Table 2 PC startup commands

Command	Result[a]
Off-2	Latching relay, inside PC, reset
On-1	PS1, 4, 8, 9, 10 turned on
On-2	PS2, 3, 7 turned on
On-3	PS5, 6 turned on; PS1 turned down to minimum

[a] For designation of the individual supplies, see Table 1.

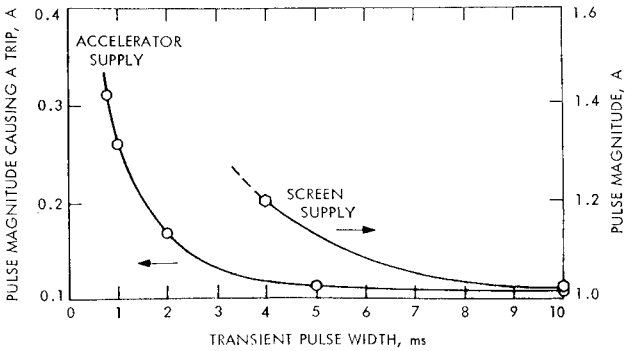

Fig. 3 Current pulse magnitude and duration causing a trip.

reduced to a minimum level and then ramped up to the original value. Both the minimum level during off time and the ramp are important for recovery.

The influence of arc current level during recycle was investigated with the thruster operating from half to full power. In contrast with the oxide cathode (BB-1), the arc must remain on during recycle of the thruster using the hollow cathode. Recycles with the arc current at its normal value and with command maximum (9amp) level were performed satisfactorily at half and full power.

The time sequence of bringing the screen and accelerator voltages back on after a trip is also important. The time between screen and accelerator turn-on was varied by delaying the accelerator turn-on command signal. Smoothest recovery was observed when the accelerator reached full voltage at least 30m faster than the screen.

4. *Cathode Keeper Current*

The HC keeper current was varied in 0.2 amp steps from 0.4–1.0 amp to evaluate arc startup and recycle. Operation at 0.4 amp was possible although the starting of the arc was somewhat delayed. Operation between 0.6 and 0.8 amp was satisfactory. At 1.0 amp, the thruster operation was "noisy" for some power ranges. A keeper current of 0.8 amp was selected.

5. *Servo Loops*

Three basic PC-thruster servo loops are used (Fig. 2) to maintain: 1) the thrust level; 2) propellant utilization efficiency; and 3) spacecraft potential. These are the screen current-main vaporizer current, arc voltage-cathode vaporizer current, and neutralizer keeper voltage-neutralizer vaporizer current servo loops, respectively. The transfer characteristics are shown in Fig. 4. These characteristics were derived by adjusting the loop gains to the maximum values not producing oscillations.

Thrust depends directly upon screen current (I_5) and the square root of screen voltage $(E_5)^{\frac{1}{2}}$. Figure 4a shows the closed-loop characteristics of the screen-main vaporizer servo system. When the beam current exceeds the reference $I_{B,R}$ value, the loop closes and the vaporizer is controlled along the S_2-slope. The exact location of the steady-state operating point on this slope depends upon a number of factors, including the beam current level, the temperature of the thruster, the condition of the vaporizer, and the over all thermal environment. As the steady-state operating point shifts along the S_2-slope, the value of the error signal, ΔI_5, changes and can become as large as 16 ma at the bottom of the curve. This means that the actual beam current can be as much as 16 ma higher than that specified by the reference $I_{B,R}$. This current variation represents a total thrust variation of ± 0.8 to $\pm 1.6\%$ at full- and half-power, respectively, provided that $I_{B,R}$ has been properly adjusted to have the steady-state operating point at the level of the desired screen current. Assuming that the average value of the vaporizer current I_2 in steady state does not change from the nominal value by more than $\pm 25\%$, the thrust variation caused by the screen current variation will be less than ± 0.2 to $\pm 0.4\%$ of the nominal value. However, the screen current variation results in an opposite propellant utilization variation since the arc power as defined by the arc current reference remains constant. Thus, the finite gain of the screen current servo loop can result in a propellant utilization variation of about ± 0.2 to $\pm 0.4\%$, when operating at maximum power and a propellant utilization efficiency of 90%.

Associated with the thrust variation is a power variation. For constant screen voltage, the change in screen current over the control range represents a ± 0.8 to $\pm 1.6\%$ screen power change. Thus, from the nominal operating point power, an additional power margin of about 15w (at 2 kv) must be

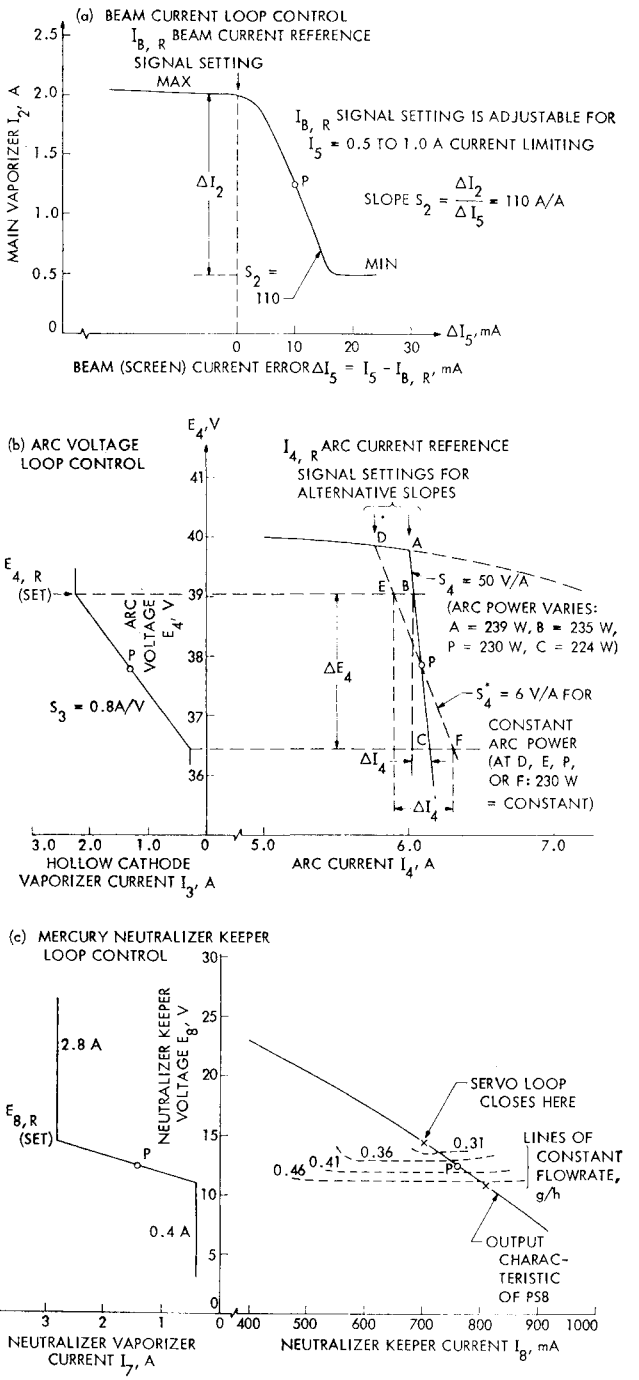

Fig. 4 Transfer characteristics.

provided in both the screen supply and the solar array. This amounts to about ± 0.64 to $\pm 1.28\%$ of the PC output power at full- and half-power, respectively.

The arc voltage-cathode vaporizer loop has the function of maintaining a reference arc voltage. The arc supply current is controlled by an adjustable arc current reference $I_{4,R}$. The reference may be adjusted internally as a function of the beam current reference signal $I_{5,R}$ or by an external command. The servo loop and arc power supply characteristics are shown in Fig. 4b. Since both the arc current and arc voltage vary as the loop controls, the evaluation of utilization variation must be made on the basis of discharge power.

A plot of arc power over the control range is shown in Fig. 4b. The solid line ($S_4 = 50$ v/A) represents the initial system characteristic and shows a total power change of about 15w over the normal control range. The arc power can be represented approximately in form[13]

$$P_A = I_5\{A_1[(p/p_t)]^{\beta_1} + A_2(1/1 - \eta_m)\} \quad (1)$$

where I_5 is screen current, A_1, A_2, and β_1 are constants, and p/p_t is the ratio of any thruster power to full rated power. The constant β_1 is small (about -0.1) for the hollow cathode. Differentiating Eq. (1),

$$dP_A = I_5 A_2 d\eta_m/(1 - \eta_m)^2 \quad (2)$$

Evaluating Eq. (2) for a nominal $\eta_m = 0.9$,

$$d\eta_m = 10^{-2} dP_A/A_2 I_5 \quad (3)$$

A typical value of A_2 is 6 ev/ion, giving

$$d\eta_m = 1.66 \times 10^{-3} dP_A/I_5$$

or approximately

$$\Delta\eta_m = 1.66 \times 10^{-3} \Delta P_A/I_5 \quad (4)$$

For the present conditions, $\Delta P_A = 15$w, so that $\Delta\eta_m = 2.5\%$ and 5.0% at full- and half power, respectively.

Three points are to be noted. First, assuming a $\pm 25\%$ variation in cathode vaporizer current I_3 due to warm-up or deterioration, causing a steady-state change in arc voltage, a utilization variation of about ± 0.35 to $\pm 0.7\%$ could be expected.

Second, dynamically the change in arc power (for $S_4 = 50$) in Fig. 4b results in a perturbation of the screen current-main vaporizer loop. This happens because the arc power supplies the screen current ions. In addition, coupling occurs in the reverse direction because the main flow affects the required cathode flow.

These control loops were originally "stabilized" by adjusting the arc voltage loop gain without the preceding analysis. Although this produced relatively well-behaved thruster operation, the system remained slightly oscillatory. A more desirable arc supply characteristic is shown as a dashed line ($S_4 = 6$) in Fig. 4b, corresponding with the constant arc power line. For this slope, the arc current level adjustment effectively becomes an arc power level adjustment. Although this will not totally eliminate loop coupling, it will eliminate direct coupling. This approach was found to substantially reduce control oscillations.

The third point is that, with the present arc supply characteristic, the steady-state operating point may be approached from both the high- and low-propellant utilization region during the steady-state oscillations. Oscillations, particularly at high screen current for which the stability margin is small, are prone to cause runaway. The constant arc power E_4/I_4 slope reduced this problem.

The neutralizer maintains a given spacecraft potential, with respect to the local space plasma, by injecting electrons into the ion beam. The electrons originate at a hollow cathode, similar to the main arc cathode, and pass through a plasma column or bridge connecting the neutralizer and ion beam. The voltage drop down this column is the coupling voltage. This coupling voltage is generally proportional to the neutralizer keeper voltage.[14] By maintaining a given keeper voltage, an adequate electron current is available for neutralization.

The present neutralizer servo loop characteristics are shown in Fig. 4c. The nominal operating point is at $E_8 = 12.5$ v and $I_8 = 0.72$ amp. The flowrate for this point is about 0.4 g/hr. This represents about 5 to 10% of the total propellant flow at full and half beam power, respectively.

Variation of the neutralizer vaporizer operating point by $\pm 25\%$ would produce a utilization efficiency change of ± 0.35 to $\pm 0.70\%$. Neutralizer tests are in progress to reduce the total propellant flow and the flow rate variation due to control loop excursions.

BB-1M Evaluation Testing

A series of tests was performed to evaluate the basic PC characteristics, independent of integration problems. The results show capabilities, limitations, and general problem areas fundamental to transistor power conditioning. Efficiency, ripple, regulation, grounding and cabling techniques (internal to PC and external) are significant in over-all system design. However, each of these must be clearly defined to avoid substantial differences in interpretation.

A. PC Efficiency

There are numerous definitions for efficiency. The definitions relating to the present work are listed below:

1) Thermal efficiency is based on heat dissipation: the ratio of PC output power to output power plus dissipation. In principle, the dissipation can be accurately measured in a calorimeter. The use of output power in both numerator and denominator reduces the effect of output power measurement errors.

2) Average volt-ampere efficiency is based on the ratio of average power out to average power in. In this case, the average is based on average reading d.c. meters for d.c. input and output and on rms meters for a.c. outputs. If the a.c. component (ripple) imposed on the d.c. values is reasonably small, and if the ripple current and voltage are in phase (nonreactive), this average *E-I* efficiency is identical with that in type 1.

3) Effective volt-ampere unit efficiency is based on the maximum required input volt-amperes, including ripple and average output power. This definition results from the fact that the power source must supply peak power, up to certain frequency limits, while thrust depends only upon average power. The difference between this efficiency and type 2 depends upon the input ripple frequency and the power source (solar array) frequency response characteristics. In addition, the solar array response depends upon power loading.[8] Near the maximum power point, ripple below about 50 kHz will affect the array. Thus, the maximum required input is the power the solar array must supply, including the amount of ripple to which the array responds.

4) Effective volt-ampere over all efficiency is an extension of type 3 to include power dissipation in cabling and connections. In total system analyses, particularly mission calculations and solar array sizing, a single efficiency (from array output to thruster input) is generally used. This value must obviously include any significant losses.

A series of efficiency measurements was made using precision d.c. meters. These were intended for PC evaluation as well as to establish a consistent method of measurement without a calorimeter. Initially, the PC full-power efficiency (type 2, preceding) was found to be $(85.2 \pm 0.2)\%$ (67-v input at PC; output at test console, including 4m of cable). The measurements were made with numerous calibrated instruments for comparison and included corrections for all

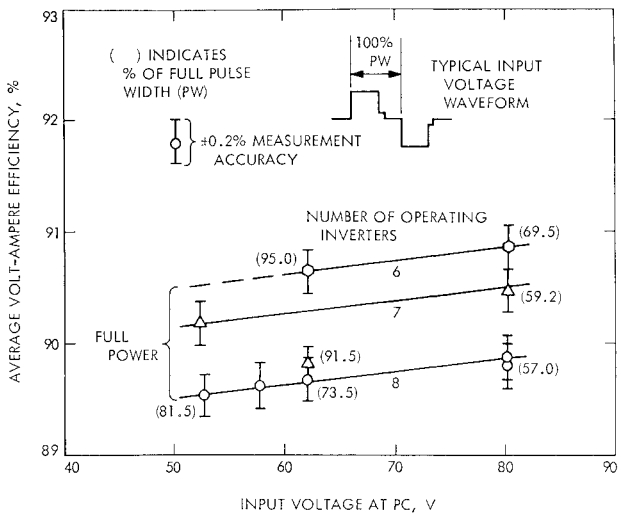

Fig. 5 Screen supply efficiency.

line voltage drops. Since this efficiency was lower than expected, a more detailed study was conducted.

Temperature measurements were made to establish relative transistor temperatures. By replacing "hot" units in screen inverter 7 with SDT 8805's, the BB-1M efficiency increased to $(85.7 \pm 0.2)\%$. Transitron transistors (ST-18037) were then substituted in the next hottest inverter (No. 3). This increased the screen supply efficiency to $(86.4 \pm 0.2)\%$.

All BB-1M screen inverters were replaced with those from EX-1. The results of this testing are shown in Fig. 5. Based on this data the EX-1 and EX-2 units were expected to yield over all efficiencies of 88.5–90% for all line voltages.¶

B. Input Ripple

Considering the previous efficiency discussion, the magnitude and frequency of the input ripple are important in over all system design. Measurements were made with an oscilloscope clamp-around current probe and a voltage probe.

For PC full-power operation, using a laboratory power supply with an input of about 45 amp at 64 v, the peak-to-peak current ripple is about 1.15 amp at 10 kHz. If the solar array voltage is assumed to remain constant with this ripple loading, the peak power demand increases by about 1.2%.

At full power with two screen inverters off, the ripple current is about 1.73 amp peak to peak at 20 kHz. This corresponds to a peak power increase of about 1.9%. The higher frequency is due to the effect of the staggered phase screen system. Without the screen supply but full power otherwise the ripple is about 2.2 amp peak to peak at 10 kHz. The final determination of the effect of ripple on over all system performance must await tests with a solar panel.

C. Output Ripple

The output ripple of most interest is that on the screen, accelerator, and arc supplies. The principal limitations on the ripple magnitude arise from power supply mutual interactions, servo loop-power supply interactions, accelerator current disturbances, and propellant utilization efficiency variations.

Voltage ripple on the screen or accelerator supply output induces a current ripple since the plasma ion source is not completely emission-limited. For a given ion optics design, the total extraction voltage $(E_5 + |E_6|)$ is chosen to draw a specified maximum beam current. Note that, for a constant arc current, the screen and accelerator currents vary with the total extraction voltage. If the total ripple $(\Delta E_5 + |E_6|)$ is greater than the voltage margin, the ion beam is defocused on half the ripple cycle. This would result in significant accelerator current variations and a reduction in propellant utilization efficiency. For the present thruster at full power, the margin is about 450 v.

Three sources of ripple on the arc output are available: 1) the supply voltage ripple (into a resistive load); 2) an oscillation in the arc plasma; and 3) coupling with the screen and accelerator ripple. Of these, the second is presently most significant and can produce a peak-to-peak current ripple of about 50% of the d.c. level. This large ripple couples directly to the screen and accelerator current. The extent of this coupling depends largely upon the average propellant utilization efficiency. If the peak ripple current cannot produce a large increase in screen current, as at high utilization, the effect will be relatively small. However, at utilizations below below 85–90%, the arc ripple will be reflected in the screen current in direct proportion to the arc d.c. level.

At full power, the peak screen current ripple effectively reduces the total ion extraction voltage $(E_5 + |E_6|)$ margin by moving the operating point to a higher level. However, when combined with the peak voltage ripple, the optics design is satisfactory. The effect of the output ripple on servo loop operation is not significant. The ripple frequency is several orders of magnitude greater than servo loop time constants.

D. Regulation

Principally, two factors must be considered in determining regulation requirements (for input line and load changes): 1) system over-all predictability for spacecraft navigation; and 2) adequate total voltage margin as discussed in the previous section. In the first category, the parameters requiring accurate control are thrust $[I_5,(E_5)^{\frac{1}{2}}]$ specific impulse $[(E_5)^{\frac{1}{2}}, \eta_m]$, and propellant utilization.

The servo loops were designed to maintain accurate control of I_5 and η_m for constant E_5 and E_6. Considering the discus-

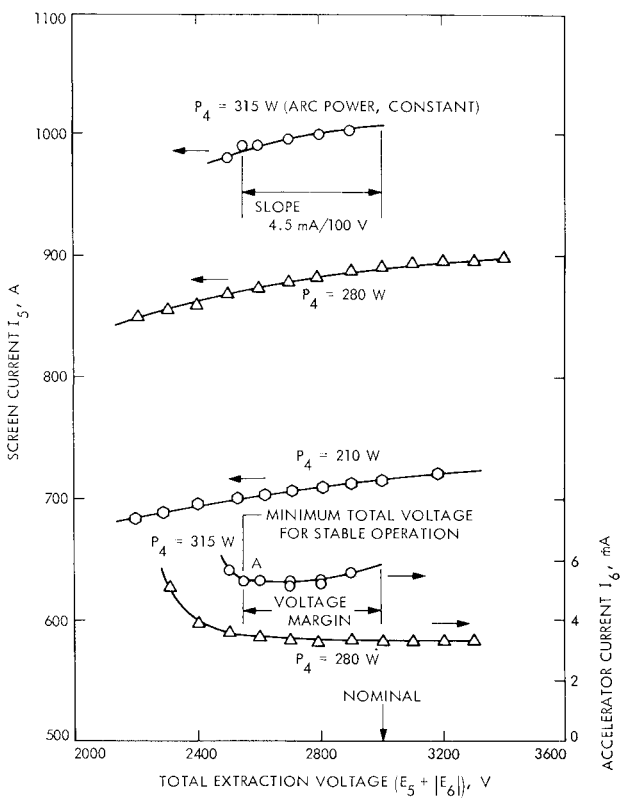

Fig. 6 Screen and accelerator current vs total extraction voltage.

¶ Subsequent testing of the EX-1 and EX-2 units with meters and with a calorimeter confirmed this prediction.

sion of Fig. 6, a change in total voltage can result in a substantial change in η_m, depending upon the magnitude of the ripple.

However, assuming operation on the right-hand portion of the curves in Fig. 6, the equivalent slope is 0.45% utilization per 100 v at full power. Thus, to maintain an accuracy of 0.1% on η_m, combined regulation of the PS5 and PS6 supplies must be better than 0.7%.

The percent regulation on E_5 is roughly double that needed on thrust and specific impulse. If the expected variation in η_m is 0.5% for 1% control on thrust and specific impulse, E_5 must be regulated to 1%. Regulation of about 0.4% (8 v) (53–80-v input and 400–1000-ma load) was provided in the present PC design. Regulation of the accelerator supply was about 1%. The combined regulation tolerance produces a change of less than 0.2% in propellant utilization efficiency. Thus, the regulation needed to satisfy spacecraft navigation requirements on η_m appears to satisfy the total voltage margin requirement as well.

E. PC Weight Analysis

A minimum mass design is of great importance in achieving full technology readiness with the PC. The BB-1M PC had a weight of 18.05 kg corresponding to about 6.7 kg/kw of input power. Substantial lightening was accomplished in the EX-1 and EX-2 units by efficient repackaging, redesign, and structural thickness reductions. The lightening program resulted in a PC weight of 13.3 kg or 4.9 kg/kw of input power. The details of the module weight breakdown for the BB-1M and EX units are presented in Ref. 15.

Summary and Conclusions**

The successful PC-thruster integration and testing described in this paper represent a milestone in the development of electric propulsion system technology. The performance goals were substantially met despite the constraints of input voltage variation and ripple. In addition, the general understanding of transistor PC operation, capabilities, and limitations has been improved. The interactions with other propulsion system elements are more clearly defined. The specific results of this work are summarized below: 1) closed-loop operation over the 2 to 1 power range was verified. Additional tests were suggested to reduce servo loop interactions. 2) Output ripple must be considered in terms of the ion optics voltage marging and power supply (PS5 and PS6) regulation. The combined PS5 and PS6 ripple and regulation must not exceed the margin (450 v in the present case) which would defocus the ion beam. 3) The expected uncertainty in level of thrust, due to variations in E_5 and I_5 due to PS5 regulation and servo loop operation, is estimated to be about ± 0.4 to ± 0.6% for full- and half-power, respectively. 4) The uncertainty in propellant utilization efficiency, due to the servo loops and PS5 regulation, is estimated to be about ± 1.1 to ± 2.0% at full- and half-power, respectively. 5) The uncertainty in specific impluse, due to the uncertainty in utilization and the regulation of PS5, is estimated to be about ± 1.3 to ± 2.2% at full- and half-power, respectively. 6) Considering conclusions 3–5, means for improving the thrust, specific impulse, and propellant utilization uncertainties should be investigated. These uncertainties were based on an arbitrarily assumed ± 25% change (due to warm-up and degradation) in the vaporizer current operating points from nominal. With accurate telemetry data for the critical parameters (E_5, I_5, E_4, I_4, E_8, I_8, I_2, I_3, and I_7) and sufficiently fine adjustment capability on $I_{4,R}$ and/or $I_{5,R}$, the uncertainties due to the servo loops could be reduced by readjusting the steady-state operating points. 7) The definition of PC "efficiency" has been clarified by proposing the use of four pertinent efficiencies. In the tests to date, a thermal efficiency (type 1) measurement has not yet been made. The average volt-ampere efficiency (type 2) of the BB-1 unit ranges from about 84.5–86.0%, depending on input voltage and the number of operating screen inverters. This efficiency is expected to go up to 88.5–90% for the EX-1 and EX-2 units. Evaluation of the effective volt-ampere unit efficiency (type 3) will require testing with an actual solar array. 8) The weight of the BB-1 unit is 18.0 kg. This value is expected to be reduced to 13.3 kg in the EX-1 and EX-2 units. Thus, a specific mass of 4.9 kg/kw will be achieved.

** During the review and editing cycle for this paper, the EX-1 and EX-2 PC units were integrated into the SEPST system. Extended testing in thermal-vacuum was accomplished with relatively minor difficulty. The conclusions stated here for the BB-1M unit are valid for the EX units including projected weight and efficiency values. Extensive data on the EX unit integration and thermal-vacuum experience will be presented in a future report.

References

[1] Kerrisk, D. J. and Kaufman, H. R., "Electric Propulsion Systems for Primary Spacecraft Propulsion," AIAA Paper 67–424, Washington, D. C., 1967.

[2] Masek, T. D. and Pawlik, E. V., "Thrust System Technology for Solar Electric Propulsion," *Journal of Spacecraft and Rockets*, Vol. 6, No. 5, May, 1969, pp. 557–564.

[3] Kerrisk, D. J. and Bartz, D. R., "Primary Electric-Propulsion Systems Technology and Applications," *Astronautics and Aeronautics*, Vol. 6, No. 6, June 1968, pp. 48–53.

[4] Macie, T. W., Pawlik, E. V., Ferrera, J. D., and Costogue, E. N., "Solar-Electric Propulsion System Evaluation," *Journal of Spacecraft and Rockets*, Vol. 7, No. 8, Aug. 1970, pp. 968–976.

[5] Pawlik, E. V., Costogue, E. N., and Schaefer, W. C., "Operation of a Lightweight Power Conditioner with a Hollow Cathode Ion Thruster," *Journal of Spacecraft and Rockets*, Vol. 8, No. 3, March 1971, pp. 245–250.

[6] Masek, T. D. and Macie, T. W., "Solar Electric Propulsion System Technology," AIAA Paper 70–1153, Stanford, Calif., 1970.

[7] Muldoon, W. J., Garth, D. R., and Benson, G. C., "Functional and Physical Design of a Flight Prototype Ion Engine Power Conditioner," ASME Paper 70-AV/SPT-38, ASME, Space Technology and Heat Transfer Conference, 1970, Los Angeles, Calif.

[8] Zerbel, D. W. and Decker, D. K., "AC Impedance of Silicon Solar Cells," IECEC Conference, Las Vegas, Nev., 1970.

[9] Cronin, D., Golding, D., and Biess, J., "Power Conditioning Suitable for High-Performance Electric Spacecraft," AIAA Paper 69–240, Williamsburg, Va., 1969.

[10] Macie, T. W. and Masek, T. D., "Power Conditioner Evaluation: Circuit Problems and Cures (SEPST III-Breadboard 1)," *Supporting Research and Advanced Development*, Space Programs Summary 37–62, Vol. III, April 30, 1970, Jet Propulsion Lab., Pasadena, Calif.

[11] Pawlik, E. V., Macie, T. W., and Ferrera, J. D., "Electric Propulsion Systems Performance Evaluation," AIAA Paper 69–236, Williamsburg, Va., 1969.

[12] Kerslake, W. R., Goldman, R. G., and Nieberding, W. C., "SERT II: Mission, Thruster Performance, and In-Flight Thrust Measurements," *Journal of Spacecraft and Rockets*, Vol. 8, No. 3, March 1971, pp. 213–224.

[13] Masek, T. D., "Sizing a Solar Electric Thrust Subsystem," 32–1504, Nov. 1970, Jet Propulsion Lab., Pasadena, Calif.

[14] Rawlin, V. K. and Pawlik, E. V., "A Mercury Plasma-Bridge Neutralizer," TM X-52335. 1967, NASA.

[15] Garth, D. R., Muldoon, W. J., and Benson, G. C., *Development and Test of a Flight Prototype Power Conditioner* for *20-cm Mercury Bombardment Electric Thruster System*, JPL Contract 952297, April 1971, Hughes Aircraft, Culver City, Calif.